XLVI CILAMCE
VITÓRIA - ES - BRAZIL - 2025
XLVI IBERO-LATIN AMERICAN CONGRESS ON COMPUTATIONAL METHODS IN ENGINEERING

# Corotational beam element for nonlinear dynamic analysis of offshore production lines

Heleno P. Bezerra Neto[1], Wydem L. E. Santos[1], Eduardo N. Lages[1]

[1]*Laboratory of Scientific Computing and Visualization, Technology Center, Federal University of Alagoas*
*Av. Lourival de Melo Mota, 57072-970, Alagoas/Maceió, Brazil*
*helenopontes@ctec.ufal.br, wydem.santos@lccv.ufal.br, enl@lccv.ufal.br*

**Abstract.** To ensure the safety and functionality of floating platforms, nonlinear dynamic analysis of mooring lines, production risers, offloading hoses, and control/service umbilicals is essential. DOOLINES, an object-oriented computational framework, performs these analyses in the time domain using the Finite Element Method (FEM). Originally, DOOLINES employed spatial truss elements with six translational degrees of freedom, which directly represented axial stiffness but only indirectly accounted for bending stiffness. This work extends the capabilities of DOOLINES through the implementation of a corotational beam element (12 degrees of freedom: 6 translations and 6 rotations), which explicitly models axial, bending, and torsional stiffness. The adopted corotational formulation enables the capture of large displacements and rotations while maintaining the assumption of small strains. Comparative simulation results with truss elements and a reference commercial software show excellent agreement, thus validating the proposed implementation. Although the new element requires greater computational resources, its comprehensive formulation proves particularly advantageous in scenarios where bending and torsional effects are significant, such as in offshore production risers.

**Keywords:** Corotational beam, Finite Element Method, Analysis of risers, DOOLINES, Nonlinear dynamics.

## 1 Introduction

Offshore oil and gas platforms are extremely important for the exploration of oil and gas around the world—commodities that are essential and key sources of energy globally. Designed according to the specific conditions of their installation site, each offshore platform is therefore unique in its design (Chandrasekaran [1]).

Essential components of these structures include mooring lines, production risers, offloading hoses, and control/service umbilicals, which play a crucial role in the development and operation of oil and gas infrastructure (Wu et al. [2]). Like the platforms themselves, these components must undergo dynamic structural analyses to ensure their performance and operational safety under environmental loads typical of the marine environment, such as wind, waves, and currents, as well as seismic activity and dead load.

Considering the need for structural analysis of these offshore platform components, the DOOLINES (Dynamics Of Offshore LINES) framework was developed, an object-oriented platform focused on the nonlinear dynamic analysis of mooring lines and offshore production systems in the time domain (Silveira et al. [3]).

In its earlier versions, DOOLINES provided only a special lumped-mass truss element with indirect consideration of bending stiffness, featuring three translational degrees of freedom per node, called BTruss. This work presents the implementation of a corotational beam element with 12 degrees of freedom, 6 translational and 6 rotational, which explicitly models axial, bending, and torsional stiffnesses, called BeamCR. This enhancement enables DOOLINES to fully capture all relevant degrees of freedom in scenarios where bending and torsion produce significant effects.

# 2 Corotational formulation

The corotational formulation was developed based on the Element Independent Corotational (EICR) formulation proposed by Nour-Omid and Rankin [4]. The idea of the method is to use an undeformed local axis system, also called the corotational system, as a reference. This system follows the element such that the displacements of the element relative to it are purely deformational. The principle of the formulation is to separate rigid body motions from deformational ones, allowing the use of linear element formulations within nonlinear analyses.

Monteiro [5] developed a corotational formulation for spatial frames based on the original approach. Subsequently, Menin [6] extended the application of the theory developed by Monteiro [5] to various structural systems, including trusses, planar frames, shells, and spatial frames. The formulation presented in this work, with few modifications, is inspired by Menin's approach.

According to Menin [6], the corotational formulation offers the advantage of not requiring internal modifications to existing linear finite element routines, since the separation between rigid body motions and deformational motions is performed through so-called projection operators (or projectors). These operators can be used as pre- and post-processors in computational routines, providing the formulation with high flexibility and ease of implementation.

## 2.1 Kinematics description

To describe the motion of a generic element, we use three reference systems: the global $xyz$, the local system (T), also called corotational system, and nodal system (A and B), as shown in Fig 1.

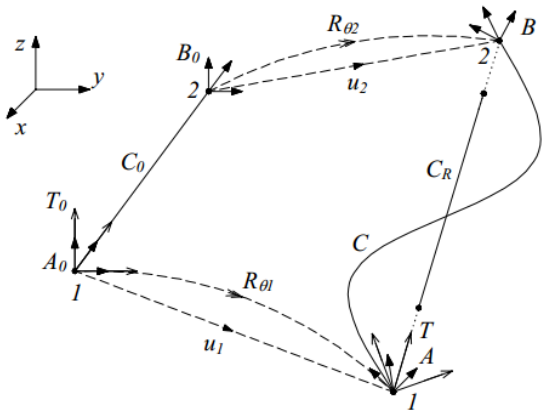



Figure 1. Initial ($C_0$), co-rotaded ($C_R$) and deformed ($C$) configuration of the beam element. Source: Menin [6]

The global system is defined by three fixed orthonormal vectors $xyz$. The local system ($T$), on the other hand, consists of orthonormal vectors that both translate and rotate with the element, with its origin located at the element's initial node. The local system is defined by

$$T = \left[ {i_1}^T \; {i_2}^T \; {i_3}^T \right], \tag{1}$$

where the vector $i_1$, represents the axial direction of the element, pointing from the initial node to the final node, while the remaining vectors are constructed as follows:

$$i_3 = \frac{i_1 \times v}{|i_1 \times v|}, \tag{2}$$

$$i_2 = i_3 \times i_1, \tag{3}$$

where $v$ is an auxiliary vector defined based on the nodal axes.

$$v = \frac{1}{2}(A + B)[0\ 1\ 0\ ]^T. \tag{4}$$

The nodal axes of the element are attached to the initial $(A)$ and final $(B)$ and define the orientation of the element's cross-section at these nodes. At the initial time, the local and nodal axes are denoted by: $T_0$, $B_0$ and $A_0$. The rotation of the nodal axes is performed using a rotation matrix.

$$A = R_{\theta 1}A_0, \qquad B = R_{\theta 2}B_0, \tag{5}$$

in which $R_{\theta 1}$ and $R_{\theta 2}$ represent the rotation matrices of the initial and final nodes, respectively, which can be defined using the Euler-Rodrigues formula.

Once the coordinate systems are defined, the deformational displacements and rotations of the element must be calculated. To do this, the transformation of coordinates from the global system to the local system must be established. Let $x_e$ be the coordinates of any node in the local system, and $x$ the corresponding coordinates in the global system. The relationship between these coordinates is given by

$$x^e = Tx. \tag{6}$$

Given that the local system has its origin at the initial node of the element, the position of the i-th node of the element relative to the local system, denoted by $x_i^c$, is defined by

$$x_i^c = T(x_i - x_1). \tag{7}$$

Thus, the deformational displacement experienced by the node in the current configuration of the element can be calculated by

$$u_i^c = T(x_i - x_1) - x_{i0}, \tag{8}$$

with $x_{i0}$ denoting the position of the i-th node in the initial configuration of the element relative to the initial local system $T_0$. Using Eq. (8) along with definition of the local system, the deformational displacements of the initial and final nodes are presented as follows

$$u_1^c = 0, \qquad u_2^c = [L - L_0\ 0\ 0\ ]^T, \tag{9}$$

where $L$ and $L_0$ represent the current and initial lengths of the element, respectively.

The deformational rotation can be calculated as follows

$$\theta_1^c = rot(TA), \qquad \theta_2^c = rot(TB), \tag{10}$$

with $\theta = rot(R_\theta)$ being operation that extracts the rotation components of $\theta$ from $R_\theta$.

### 2.2 Internal forces

The internal forces of the element, in the local system, are calculated assuming a linear relationship between stress and strain valid for small displacements and rotations. Under this assumption, the classical stiffness matrix of the beam element according to Euler-Bernoulli theory can be used. Thus, the internal forces in the local system can be calculated using the following equation:

$$f_e = K_e u_e, \tag{11}$$

where $K_e$ is the element stiffness matrix, and $u_e$ are the local deformational displacements of the element, defined as:

$$u_e = [u_1^c\ \theta_1^c\ u_2^c\ \theta_1^c\ ]^T. \tag{12}$$

The internal forces in the global system are then calculated as

$$f = T_{LG}T_e^{-T}f_e, \tag{13}$$

with $T_{LG}$ being the transformation matrix from the local to the global system, and $T_e$, according to Wang et al. [7], a 12×12 matrix defined as:

$$T_e = \mathrm{diag}[I \quad T(\theta_1^c) \quad I \quad T(\theta_2^c)], \tag{14}$$

where T(θ) is a tangential transformation operator defined as:

$$T(\theta) = I + \frac{1 + cos\ cos\ (|\theta|)}{|\theta|^2} S_\theta + \frac{|\theta| - sin\ (|\theta|)}{|\theta|^3} S_\theta S_\theta, \tag{15}$$

with $\theta$ being the rotation vector $\theta$, and $S_\theta$ is the skew-symmetric matrix associated with the vector $\theta$.

### 2.3 Mass matrix

For the calculation of the mass matrix components of an element with a hollow circular cross-section filled with fluid, only half of the finite element was considered. The components of the global velocity vector at any point, expressed as functions of the global coordinates, are given by:

$$\frac{dU}{dt} = v_x + z\omega_y - y\omega_z, \tag{16}$$

$$\frac{dV}{dt} = v_y - z\omega_x + x\omega_z, \tag{17}$$

$$\frac{dW}{dt} = v_z + y\omega_x - x\omega_y, \tag{18}$$

where $U$, $V$ and $W$ represent the displacements along the global $x$, $y$ and $z$ axes, respectively, while $v_i$ and $\omega_i$ denote the linear and angular velocities of the node in the global i-direction, respectively, and $t$ is time.

The specific kinetic energies of the element and the internal fluid are given by:

$$T0_E = \int_\Omega \frac{1}{2}\rho_E \left(\frac{dU^2}{dt} + \frac{dU^2}{dt} + \frac{dW^2}{dt}\right) d\Omega, \tag{19}$$

$$T0_F = \int_\Omega \frac{1}{2}\rho_F \left(\frac{dU^2}{dt} + \frac{dU^2}{dt} + \frac{dW^2}{dt}\right) d\Omega, \tag{20}$$

with $T0_E$ and $T0_F$ denoting the specific kinetic energies of the element and the fluid, respectively. Likewise, $\rho_E$ and $\rho_F$ represent the densities of the element and fluid, respectively, and $\Omega$ stands for the volume.

The mass matrix is obtained from the Hessian matrix of the kinetic energy with respect to the terms $v_x$, $v_y$, $v_z$, $\omega_x$, $\omega_y$, $\omega_z$. To perform the diagonalization of the matrix, the HRZ method (Hinton, Rock, and Zienkiewicz [8]) was used, with the components of the lumped mass matrix given by:

$$M_1 = M_2 = M_3 = \frac{L_0(\rho_E A_E + \rho_F A_F)}{2}, \tag{21}$$

$$M_4 = \rho_E L_0 \left(\frac{A_E\left(1 - i_{1_x}^2\right)L_0^2}{12} + I_E\left(1 - i_{3_z}^2\right)\right) + \rho_F L_0 \left(\frac{A_F\left(1 - i_{1_x}^2\right)L_0^2}{12} + I_F\left(1 - i_{3_x}^2\right)\right), \tag{22}$$

$$M_5 = \rho_E L_0 \left(\frac{A_E\left(1 - i_{1_y}^2\right)L_0^2}{12} + I_E\left(1 - i_{3_y}^2\right)\right) + \rho_F L_0 \left(\frac{A_F\left(1 - i_{1_y}^2\right)L_0^2}{12} + I_F\left(1 - i_{3_y}^2\right)\right), \tag{23}$$

$$M_6 = \rho_E L_0 \left(\frac{A_E\left(1 - i_{1_z}^2\right)L_0^2}{12} + I_E\left(1 - i_{3_z}^2\right)\right) + \rho_F L_0 \left(\frac{A_F\left(1 - i_{1_z}^2\right)L_0^2}{12} + I_F\left(1 - i_{3_z}^2\right)\right), \tag{24}$$

where $M_1$, $M_2$ and $M_3$ are the mass components associated with the translational degrees of freedom, and $M_4$, $M_5$ and $M_6$ are the mass components associated with the rotational degrees of freedom. The quantities $A_E$ and $I_E$ represent the area and moment of inertia of the solid portion of the element's cross-section, respectively. $A_F$ and $I_F$ are, respectively, the area and moment of inertia of the hollow portion of the element's cross-section, which is filled with fluid.

Thus, the following diagonal mass matrix is obtained:

$$M = diag[M_1\ M_2\ M_3\ M_4\ M_5\ M_6\ ], \tag{25}$$

# 3 Numerical Model

To evaluate the performance analysis of the element developed in DOOLINES, a hose simulation is performed, and it is modeled in Chinese lantern configuration. The hose is formed by three types of materials, whose characteristics are presented in Tab. 1.

Table 1. Characteristics of materials

| Parameter | Material 1 | Material 2 | Material 3 |
|---|---|---|---|
| Outer Diameter | 0.800 m | 1.250 m | 0.800 m |
| Inner Diameter | 0.486 m | 0.486 m | 0.486 m |
| Bending stiffness ($EI$) | 0.486 m | 0.486 m | 0.486 m |
| Axial stiffness ($EA$) | 220.0 kN · m$^2$ | 230.0 kN · m$^2$ | 180.0 kN · m$^2$ |
| Torsional stiffness ($GJ$) | 6600.0 kN | 6700.0 kN | 6600.0 kN |

The model is simulated in DOOLINES considering the BeamCR and BTruss elements, also being simulated in OrcaFlex software. The three models use the same discretization of the hose, with 42 elements being used. Fixed ends are considered, and environmental actions, current and wave are considered.

A linear current profile is considered with a speed of 0.75 m/s at surface and 0.15 m/s at a depth of 21.5 m, with a propagation angle of 350°. The regular Airy wave is also considered, with a height of 8.0 m, a period of 10.0 s and an angle of incidence of 350°.

The hose is assumed to have its translational displacements restricted at the ends. In the first scenario, referred to as Case 1, the end of the hose is modeled with a pin support. In the second scenario, Case 2, the hose is modeled with fixed supports at the ends, introducing significant torsional effects due to the additional constraint.

# 4 Results

Figures 2 and 3 show the variation of effective tension and bending moment over time at the midpoint of the hose for Case 1. The results demonstrate good agreement and convergence between the simulations performed using DOOLINES and OrcaFlex. A stronger similarity is observed between the BeamCR and BTruss elements when compared to OrcaFlex, indicating consistent behavior between the two DOOLINES element types.

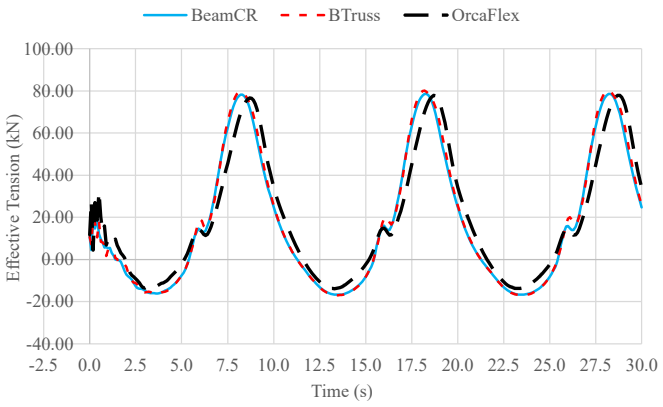



Figure 2. Effective tension at the middle of the hose for case 1.

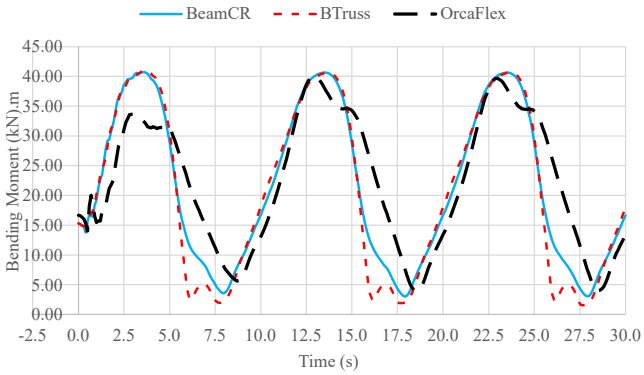



Figure 3. Bending moment at the middle of the hose for case 1.

The hose is then simulated with the fixed ends, Case 2, in which case the torsion effect is significant. Figures 4-6 show the variation of effective tension, bending moment, and torsion moment over time at the midpoint of the hose for Case 2.

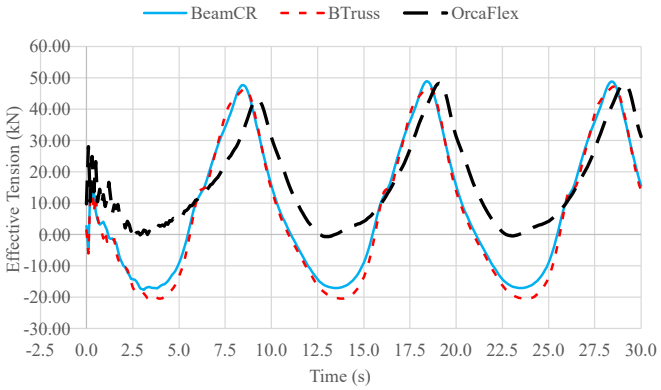



Figure 4. Effective tension at the middle of the hose for case 2.

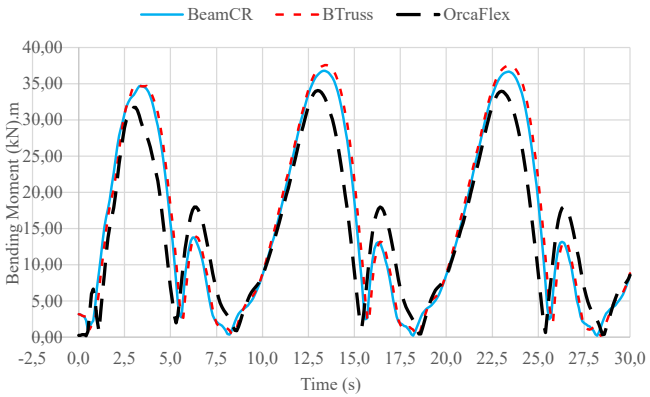



Figure 5. Bending moment at the middle of the hose for case 2.

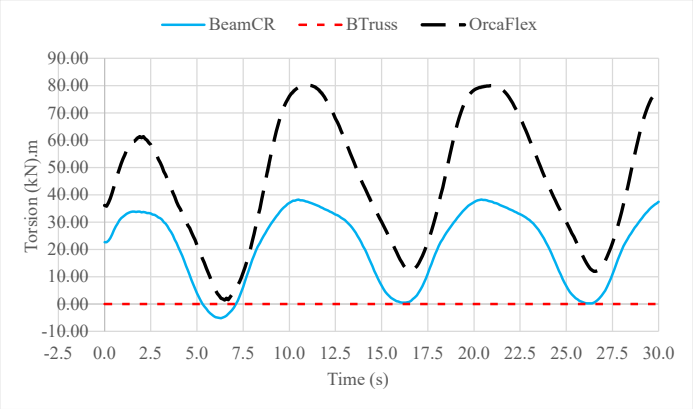



Figure 6. Torsion moment at the middle of the hose for case 2.

It is observed that all curves exhibit similar behavior, showing comparable peak values for the three models in Case 2. The similarity between the results from BeamCR and BTruss is particularly noticeable. Since the BTruss element lacks a degree of freedom to capture torsional forces, the corresponding values are zero. In contrast, BeamCR and OrcaFlex account for these forces, producing curves that are in phase with each other, although the magnitudes of their peaks and valleys differ.

## 5 Conclusions

It can be concluded that the BeamCR element developed in DOOLINES shows good agreement when compared to the BTruss element, also present in DOOLINES, and the element of the OrcaFlex software. It is verified that for the fixed ends case, the consideration of torsion becomes important, especially for production lines such as production risers and hoses.

**Acknowledgements.** The authors acknowledge PETROBRAS and CNPq for their financial support.

**Authorship statement.** The authors hereby confirm that they are the sole liable persons responsible for the authorship of this work, and that all material that has been herein included as part of the present paper is either the property (and authorship) of the authors, or has the permission of the owners to be included here.

## References

[1] S. Chandrasekaran. *Advanced marine structures*. CRC Press, 2015.
[2] W. Wu, Y. Zhao, Y. Gou, B. Lyu, Q. Lu, Z. Lu and J. Yan. An overview of structural design, analysis and common monitoring technologies for floating platform and flexible cable and riser. *China Ocean Engineering*, v. 36, n. 4, p 511-531, 2022.
[3] E. S. S. Silveira et al. DOOLINES: an object-oriented framework for non-linear static and dynamic analyses of offshore lines. *Engineering with Computers*, v. 28, p. 149-159, 2012.
[4] B. Nour-Omid and C. Rankin, "Finite rotation analysis and consistent linearization using projectors," *Computer Methods in Applied Mechanics and Engineering*, vol. 93, no. 3, pp. 353–384, 1991.
[5] F. A. C. Monteiro, Uma formulação co-rotacional: Aplicação a pórticos espaciais. MSc Dissertation, Aeronautics and Mechanical Engineering Program, Instituto Tecnológico de Aeronáutica, São José dos Campos, 2004.
[6] R. C. G. M. Menin, *Aplicação da descrição cinemática co-rotacional na análise não linear geométrica de estruturas discretizadas por elementos finitos de treliças, vigas e cascas*. PhD Thesis, Department of Civil and Environmental Engineering, Faculty of Technology, University of Brasília, Brasília, 2006.
[7] G. Wang, Z. Qi and J. Xu. A high-precision co-rotational formulation of 3D beam elements for dynamic analysis of flexible multibody systems. *Computer Methods in Applied Mechanics and Engineering*, v. 360, p. 112701, 2020.
[8] E. Hinton, T. Rock e O. C. Zienkiewicz. A note on mass lumping and related processes in the finite element method: 3F, 1T, 13R. *Earthquake Engineering & Structural Dynamics*, v. 4, n. 3, p. 245–249, 1976.